Confined Dynamics and Crystallization in Self-Assembled Alkyl Nanodomains

Shireesh Pankaj and Mario Beiner*

Naturwissenschaftliche Fakultät II, Martin-Luther-Universität Halle-Wittenberg, D-06099 Halle an der Saale, Germany

Received: August 3, 2010; Revised Manuscript Received: October 1, 2010

Long alkyl groups are used in many functional polymers to improve their performance. The methylene sequences usually show a strong tendency to aggregate to form small alkyl nanodomains which can be either completely amorphous or partly crystalline. The influence of main chain packing, domain size, and density on the properties of self-assembled alkyl nanodomains is studied on the basis of a comparison of regiorandom and regioregular poly(3-alkylthiophenes) (P3ATs) with different side-chain length as model systems. We show that the dynamics of the CH_2 units in amorphous alkyl nanodomains is mainly independent of the packing of the main chains. Relaxation spectra show a similar CH_2 dynamics despite the fact that the thiophene main chains are crystalline in regioregular but amorphous in regiorandom P3ATs. The systematic dependence of the CH_2 dynamics on alkyl nanodomain size without clear change of the average volume per CH_2 unit underlines the importance of geometrical confinement. A competition of main- and side-chain crystallization mechanisms is discussed which should be considered if higher P3ATs are optimized for optoelectronic applications.

Introduction

Functional polymers containing long alkyl groups are widely used and have been proposed as building blocks of self-assembled model systems with well-defined structures on the nanoscale having fascinating properties.[1,2] The aggregation of alkyl groups to small alkyl nanodomains with typical dimensions in the range of 10−30 Å is a general phenomenon which appears in various polymers containing long methylene sequences.[3−9] Aggregation occurs not only in the case of crystalline methylene sequences but interestingly also for alkyl groups in the amorphous state. This has been shown in particular for comblike polymers with not too long alkyl groups where side-chain crystallization is normally depressed due to frustration effects introduced by the main chains. A separation of main- and side-chain parts occurs commonly in such samples. This phenomenon has been called nanophase separation[7,8] and is found for various polymer series with $C = 4-12$ alkyl carbons per side chain attached to main chains with variable microstructure and softening behavior.[10] The long-range order in amorphous nanophase-separated side-chain polymers is usually weak but increases significantly if the side chains are long and flexible enough to crystallize far away from the main chains.[11]

Alkylated polythiophenes are of great importance as conducting polymers for modern electronic and optoelectronic applications[12−15] but also nice model systems to study the nanophase separation in comblike polymers. The microstructure of poly(3-alkylthiophenes) (P3ATs) is quite similar to that of other nanophase-separated side-chain polymers and a segregation of main- and side-chain parts on the nanoscale is observed. The alkyl groups are attached here in order to improve the processability of the materials. Specialty in the case of P3ATs is that the thiophene rings can either crystallize or remain amorphous depending on the head-to-tail arrangement of their monomeric units along the main chain (Figure 1a). Hence, P3ATs are favorable candidates to study the influence of main chain crystallization and long-range order on the properties of alkyl nanodomains.

In the case of regiorandom (rran) P3ATs, the monomers are attached statistically with either head or tail to an existing chain during polymerization. Hence, the distances between the alkyl groups along the main chain are random and the thiophene rings are not able to crystallize. As long as the side chains are not too long ($6 \leq C \leq 10$), the main and side chains remain completely amorphous and structural features as well as overall behavior of rran P3ATs are quite comparable to those of other amorphous nanophase-separated side-chain polymers like higher poly(*n*-alkyl methacrylates) or poly(*n*-alkyl acrylates).[10,16] A sketch showing the local packing of such rran P3ATs is shown in Figure 1a, case **mAsA**. Nanophase separation is indicated by (i) relatively broad prepeaks in X-ray diffraction data at scattering vectors in the range $0.2 \leq q \leq 0.6$ Å^{-1} and (ii) main-chain-independent dynamics within the alkyl nanodomains indicated by an α_{PE} process in the relaxation spectra at low temperatures which appears for different side-chain polymers containing alkyl groups with identical length at a very similar frequency temperature position.[8,10,17] It has been demonstrated that the α_{PE} process in nanophase-separated systems with longer alkyl groups ($6 \leq C \leq 12$) shows typical features of a polyethylene-like glass transition like a non-Arrhenius-like temperature dependence of the relaxation time, calorimetric activity and weak dielectric response.[10] Side-chain crystallization appears for rran P3ATs with $C > 10$ alkyl carbons per side chain (Figure 1a, case **mAsC**). Similar observations exist for other polymer series. A peculiar finding for rran P3ATs is that polymorphism has been observed.[18] The methylene units in poly(3-dodecylthiophene) (P3DDT, $C = 12$) can obviously pack on different lattices like in alkanes or polyethylene.[19,20]

In regioregular (rreg) P3ATs with >97% HT-HT sequences, the thiophene rings are able to pack on a crystalline lattice due to a highly regular attachment of their side chains to the backbone.[15,21] This improves the planarity of the thiophene rings

* To whom correspondence should be addressed. E-mail: beiner@physik.uni-halle.de. Phone: +49-345-5525350. Fax: +49-345-5527351.

10.1021/jp1072999
Published on Web 11/04/2010

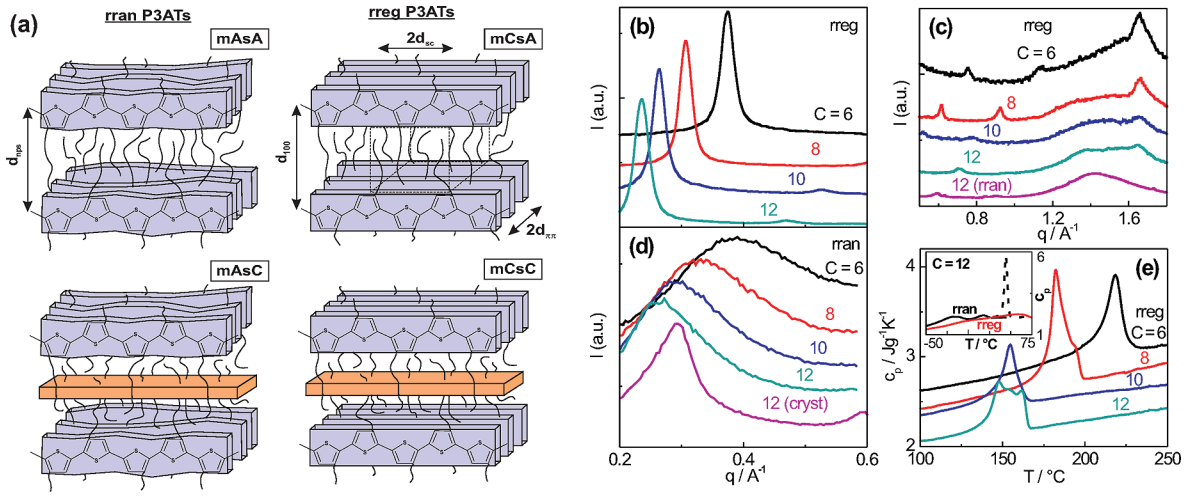

Figure 1. (a) Classification scheme for nanophase-separated side-chain polymers with main (m) and side (s) chains which can appear in the amorphous (A) or the crystalline (C) state. (b) Scattering intensity I vs scattering vector in the intermediate range 0.2 Å^{-1} ≤ q ≤ 0.6 Å^{-1} and (c) wide-angle diffraction pattern for a series of rreg P3ATs. Data for rran P3DDT (C = 12) with partly crystalline side chains are added in part (c). (d) Scattering pattern in the intermediate q range for rran P3ATs. All measurements are performed at room temperature (24 ± 1 °C). (e) DSC heating scans (dT/dt = +20 K/min) for a series of melt-quenched rreg P3ATs. The labels indicate the number of alkyl carbons per side chain C. The inset of part (e) shows DSC heating scans (dT/dt = +20 K/min) for melt-quenched rreg and rran P3DDTs in the range where side-chain crystals melt. Dotted line indicates the side-chain melting for an as-received rran P3DDT with ≈10% crystalline CH_2 units.[18]

and the overlap of their π orbitals which is a central requirement for efficient electronic charge transport.[22,23] Hence, rreg P3ATs are preferred for the application as organic semiconductors. Although rreg P3ATs are extensively investigated, there are still open questions in the discussion about their crystalline state which depends on many factors like molecular weight, sample preparation, and annealing procedure. In particular, the packing of the side chains in rreg P3ATs is not finally understood. There is still no consensus to what extent the alkyl groups are amorphous or crystalline (Figure 1a, cases **mCsA** and **mCsC**), in which way they can pack and to what extent changes in side-chain packing influence overall structure and macroscopic properties. Melting of the alkyl groups in the temperature range 30−70 °C has been reported for rreg poly(3-dodecylthiophene) (P3DDT, C = 12) in combination with changes of their optoelectronic properties.[24,25] Similar effects seem to appear for rreg poly(3-hexylthiophene) (P3HT, C = 6).[26−28] This shows clearly that a better understanding of the behavior of the alkyl groups is of central importance for the application of P3ATs.

We will show in this article on the basis of a comparison of structural and dynamic data for rran and rreg P3ATs that the alkyl groups in melt-quenched stripes of rreg P3ATs with high molecular weight and 6 ≤ C ≤ 10 alkyl carbons per side chain are basically amorphous. Weak side-chain crystallization is only observed for melt-quenched P3DDTs (C = 12). Interestingly, the α_{PE} dynamics in amorphous alkyl nanodomains of rran and rreg samples is quite comparable, although the long-range order in rreg P3ATs is significantly improved due to main-chain crystallization. The knowledge about the lattice parameters of the crystalline thiophene rings surrounding the amorphous alkyl nanodomains in rreg P3ATs is used to estimate the average volume per CH_2 group. This allows to separate the influence of average density and geometrical confinement on the dynamics of amorphous alkyl nanodomains with typical dimensions in 10−20 Å range.

Experimental Section

Samples. Two series of P3ATs with different regularity and C = 6−12 carbon atoms per side chain are studied. The rreg samples contain >97% HT-HT sequences while rran samples contain equal amounts of all possible head tail sequences (HT-HT:TT-HT:HT-HH:TT-HH). Samples were purchased from Rieke Metals Inc. Their synthesis is described in ref 29. The molecular weights as obtained from gel permation chromatography measurements against polystyrene standards are listed in Table 1. Note that this method gives usually values which are larger than the true molecular weights.[30]

TABLE 1: Sample Characterization

label	C	M_n (kg/mol)	M_w/M_n	d_{nps} or d_{100} (Å)	$T_{\alpha,10rad/s}$[a] (°C)	$T_{\alpha_{PE},10rad/s}$[a] (°C)
rreg P3HT	6	12.3	2.1	17	14	−99
rreg P3OT	8	24.3	1.6	21	−5	−88
rreg P3DT	10	92.2	1.8	24	−10	−62
rreg P3DDT	12	27.3	2.2	27	−15	−44
rran P3HT	6	31.5	2.6	16	12	−90
rran P3OT	8	19.3	3.0	20	−13	−65
rran P3DT	10	24.8	2.5	21	−25	−59
rran P3DDT	12	33.1	2.3	24	−18	−49

[a] Typical uncertainties for the estimated relaxation temperatures are ±3 K.

Experimental Techniques. X-ray scattering measurements in the range of 0.2 Å^{-1} ≤ q ≤ 0.6 Å^{-1} were performed on an instrument assembled by JJ X-rays based on a 2D detector Bruker Hi-Star and a Rigaku rotating anode. Wide-angle X-ray diffraction measurements on P3AT samples are performed using a Siemens D5000 powder diffractometer with germanium monochromator. Cu Kα radiation was used in both cases. A Rheometrics RDAII was used for dynamic shear measurements in the frequency range 0.1−100 rad/s in strip geometry (18 × 4 × 1 mm^3) with a control strain of 0.1%. DSC heating scans with a rate of 20 K/min were performed on a Perkin-Elmer DSC7. Samples with a mass of ≈5 mg have been used. All P3ATs were pressed for 30 s in the molten state (20 K above the melting point for rreg samples and at 100 °C for rran samples) into stripes which are then rapidly cooled to room temperature with an approximate rate of 50 K/min.

Results

Scattering experiments on rreg and rran P3ATs with 6 ≤ C ≤ 12 alkyl carbons per side chain in the intermediate q range

($0.2\ \text{Å}^{-1} \leq q \leq 0.6\ \text{Å}^{-1}$) are performed to study the packing of main and side chains. The pattern for all investigated rreg P3ATs (Figure 1b) show expectedly (100) reflections in this q range as well as higher order reflections (200) and (300) at larger q values (Figure 1c), indicating a lamellar morphology formed by stacked thiophene and alkyl nanodomains. All reflections (100), (200), and (300) shift systematically to smaller q values if the side-chain length increases. Spacings range from 17 to 27 Å according to Braggs law $d_{100} = 2\pi/q_{100}$ (Table 1). The average correlation length related to the (100) reflections in our rreg P3ATs is ≈240−270 Å as estimated based on Scherrer's equation.[31]

Crystallization of thiophene main chains in rreg P3ATs is confirmed by narrow reflections in wide-angle X-ray diffraction data (Figure 1c) and melting peaks in DSC scans at high temperatures $T_m \gg 100$ °C (Figure 1e). Structural perfection results in good conductivity of these samples. Consistent with literature results for rreg P3ATs,[13,32] we find that the crystalline thiophene rings show a $\pi\pi$ stacking of about $d_{\pi\pi} = 3.80 \pm 0.01$ Å which is nearly independent of side-chain lengths. The distance between the alkyl groups in main-chain direction is quite similar ($d_{sc} = 3.88$ Å). Wide-angle X-ray scattering pattern obtained at room temperature show basically only one common peak at 1.65 Å^{-1} (Figure 1c) for the (020) and (002) reflections corresponding to $d_{\pi\pi}$ and d_{sc} which is dominated by (020) contributions.[33] On the basis of the information about the distances between thiophene main chains in (100) direction and the assumption[34] that they form small crystalline plates with a thickness of about 6 Å, one can estimate the average volume per methylene unit in the alkyl nanodomains V_{CH2}. The volume of the cell indicated in Figure 1a (case **mCsA**) by dashed lines can be calculated using $V_{cell} = (d_{100} - 6\ \text{Å}) \cdot 2d_{\pi\pi} \cdot 2d_{sc}$. Considering the number of side chains entering the cell, one gets the average volume per methylene unit from $V_{CH2} = V_{cell}/4C$. The obtained values are $26.3 \pm 0.7\ \text{Å}^3$ for all investigated rreg P3ATs and larger than those of crystalline methylene units in lipids (24−25.5 Å^3)[35] and polyethylene (23.4 Å^3).[36] Obviously, the average packing density of the CH_2 units determines to a major extent the thickness of the alkyl nanodomains. The distances between the attachment points of the alkyl groups on the thiophene backbones are practically fixed since $d_{\pi\pi}$ and d_{sc} do not vary significantly with side-chain length. The consequence of an increasing side-chain length is then a nearly linear increase in d_{100} related to a thickening of the alkyl nanodomains. According to the discussed picture, a linear increase appears as the average volume per CH_2 unit is nearly constant.[37]

Looking on the scattering pattern for melt-quenched rran P3ATs with $C = 6-12$ alkyl carbons (Figure 1d), there is only one relatively broad prepeak appearing at comparable q values like the (100) reflections for corresponding rreg P3ATs. The shift of the peak maximum with side-chain length is similar for both series. This indicates that there is still a demixing of main- and side-chain parts in regiorandom P3ATs driven by the strong tendency of the alkyl groups to aggregate to form small alkyl nanodomains. The large width of the prepeak shows that the long-range order of the underlying structure is much less pronounced. The absence of higher order peaks in regiorandom P3ATs is typical for nanophase-separated side-chain polymers in the amorphous state and indicates that the interfaces between main- and side-chain domains are broad. The underlying superstructure is only short-range ordered. Correlation lengths for nanophase-separated rran P3ATs are about 4−5 times smaller than that for rreg P3ATs. DSC scans for melt-quenched rran P3ATs with $6 \leq C \leq 10$ show that these samples are fully amorphous.[18]

Results for rran P3DDT ($C = 12$) in different states underline the influence of side-chain crystallization on the overall structure of P3ATs. DSC scans for as-received samples and samples stored for many hours at temperatures in the range $-25 \leq T_c \leq 26$ °C show significant melting peaks at temperatures between −15 and 50 °C (inset Figure 1e) which are depressed in melt-quenched samples.[18] The prepeaks in the scattering pattern of semicrystalline rran P3DDT samples are sharper (Figure 1d) and higher order reflections appear (Figure 1c) similar to those for rreg samples due to crystallization of methylene units in alkyl nanodomains (in different polymorphic forms[18]). Note that DSC heating scans for melt-quenched rreg P3DDT (inset Figure 1e) also show a weak melting peak at similar temperatures as rran P3DDT, indicating the presence of crystalline methylene units in the side chains.[24,25] This underlines the existence of similarities in the side-chain behavior of rran and rreg P3ATs. However, the percentage of crystalline methylene units is small for both P3DDTs. About 10% of the CH_2 units are crystalline for rran P3DDT.[18] Although the alkyl groups are not completely crystalline in these samples, the correlation length of such semicrystalline rran P3DDTs as determined from the width of the (200) reflection is about 150 Å, i.e., much larger than that for fully amorphous rran P3ATs. This shows that the crystallization of thiophene rings as well as alkyl groups forces long-range order similarly. Nanophase separation of main and side chains, however, appears already in completely amorphous systems with less pronounced long-range order like rran P3ATs with $6 \leq C \leq 10$.

Separation of thiophene and alkyl nanodomains in both series, rreg and rran P3ATs, is strongly supported by a comparison of their relaxation behavior (Figure 2a). Surprisingly, the main features of the shear relaxation curves are quite comparable for these structurally different systems. Two prominent relaxation processes are observed in all samples. An α_{PE} process occurs at low temperatures and the conventional α relaxation process incorporating the thiophene rings at higher temperatures. The α_{PE} process is shifting to higher temperatures with increasing side-chain length while the trend for the α process is opposite. The decrease of the α relaxation temperature $T_{\alpha,10rad/s}$ taken from the isochrones is comparable to the T_g reduction seen in DSC scans for rran P3ATs[38] and can be explained like in poly(*n*-alkyl methacrylates) and other side-chain polymers by internal plasticization effects[17,39,40] caused by highly mobile alkyl side chains in the environment of the main chains. The frequency temperature positions of the α_{PE} processes in rreg P3ATs are comparable to those in rran P3ATs containing alkyl groups with identical length as well as those for many other nanophase-separated side-chain polymers (Figure 2b).[10] This confirms nicely that the α_{PE} process is related to a dynamics within alkyl nanodomains which is basically main-chain independent. Fact is that the α_{PE} processes in rran P3ATs, where the thiophene rings are amorphous, as well as those in rreg P3ATs, where the thiophene rings are highly crystalline, are similar. This finding is strengthening the nanophase separation picture and shows a high degree of independence of alkyl nanodomains. A similar shape and intensity of the α_{PE} process would not be found if the side-chain dynamics would strongly depend on the crystalline state of the thiophene rings in their environment. This statement holds even considering the recent observation that not all thiophene rings are crystalline in rreg P3ATs.[28,41−43] The main difference between the relaxation spectra is that the intensities of the α processes in rreg P3ATs have a significantly

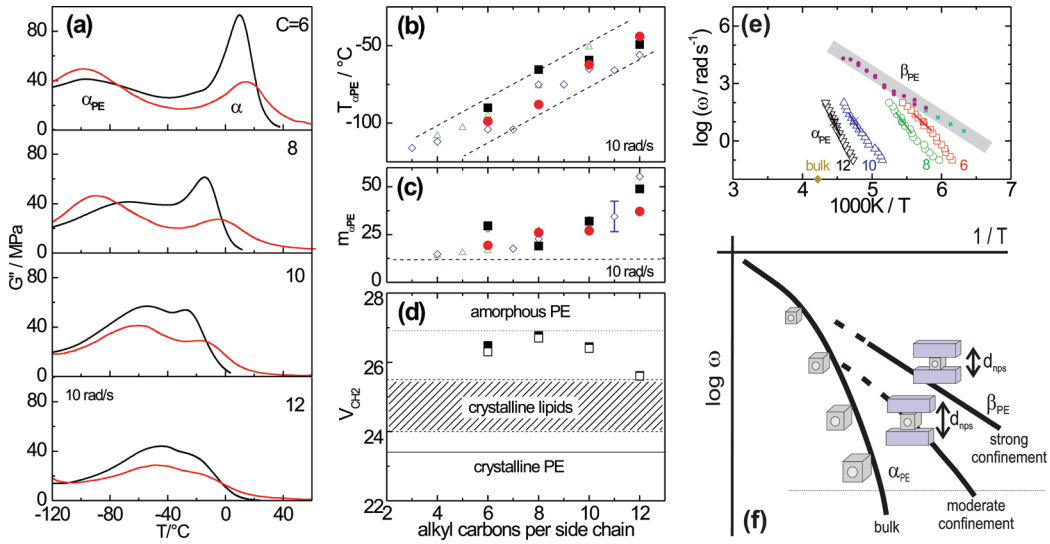

Figure 2. (a) Shear loss modulus G'' vs temperature for rran (black lines) and rreg (red lines) P3ATs measured at a frequency of $\omega = 10$ rad/s. (b) Relaxation temperatures of the α_{PE} process in the alkyl nanodomains and (c) steepness index $m_{\alpha_{PE}}$ vs C number for rreg P3ATs (circles), rran P3ATs (squares), poly(n-alkyl methacrylates) (diamonds), and poly(n-acryl acrylates) (triangles).[10] (d) Average volume per methylene unit V_{CH2} vs number of alkyl carbons per side chain C for rreg P3ATs. Full symbols are the results from calculations based on our data given in Table 1 and the main text. Open symbols correspond to calculations based on data reported in ref 32. V_{CH2} values for crystalline polyethylene (solid line),[36] amorphous polyethylene (dotted line)[62] and crystalline methylene units in lipids (shadowed area)[35] are given for comparison. All values are for ambient conditions. (e) Arrhenius plot showing the temperature dependence of the α_{PE} process in rreg in P3ATs with different side-chain length. The labels indicate the number of alkyl carbons C. The slopes used for the determination of $m_{\alpha_{PE}}$ are shown as short solid lines. Dielectric data for the Arrhenius-like β_{PE} process in poly(n-alkyl acrylates) with short side chains ($C = 4$, full squares and $C = 5$, full circles)[10] as well as the estimated glass temperature of bulk amorphous polyethylene (full diamonds)[63] are shown for comparison. (f) Scheme showing the predictions of the hindered glass transition picture for the cooperative dynamics of confined systems.[10,50]

lower intensity and that their maxima are slightly shifted to higher temperatures compared to corresponding rran P3ATs. This is an expected finding considering the fact that a large fraction of the thiophene rings in rreg P3ATs are packed on a crystalline lattice. The negligible change in the α_{PE} peak intensity for rreg P3ATs compared to their melt-quenched rran counterparts strongly confirms that the fraction of crystalline methylene units in these samples is small. Slightly broader α_{PE} peaks in rran P3ATs may indicate the existence of wider interfacial regions or certain density gradients within the alkyl nanodomains. Note that the steepness index for the α_{PE} process $m_{\alpha_{PE}} = -\mathrm{d}\log\omega/\mathrm{d}(T_{\alpha_{PE},10rad/s}/T)|_{T=T\alpha_{PE},10rad/s}$ increases systematically with increasing number of carbons per side chain C and alkyl nanodomain size d_{nps} or d_{100} like for other series of nanophase-separated side-chain polymers (Figure 2c).[10] This corresponds to a transition from Arrhenius to non-Arrhenius behavior[44] which can be also directly seen if the α_{PE} relaxation temperatures from shear measurements at different frequencies are plotted (Figure 2e). Large $m_{\alpha_{PE}}$ values for P3ATs with long alkyl groups can be understood as a clear hint for a cooperative nature of the underlying α_{PE} motions in the alkyl nanodomains. Arrhenius-like behavior with $m_{\alpha_{PE}} \approx m_{\beta_{PE}} \approx 13$ is approached for short side chains ($C \approx 6$) corresponding to more localized Johari−Goldstein[45] like motions, i.e., a β_{PE} process as discussed recently for poly(n-alkyl methacrylates).[16,44,46]

Discussion

The state of the side chains in rreg P3ATs is controversially debated since this interesting class of materials was discovered. For the lower members, situations ranging from fully amorphous to completely crystalline alkyl groups have been considered as discussed in ref 47. Side-chain melting is usually reported for rreg P3DDT ($C = 12$)[24] and members with even longer side chains. Hence, it is sometimes discussed that only methylene units far away from the backbone do crystallize.[24,48] This view is supported by our observations. From a comparison of shear, DSC, and X-ray scattering data for rreg and rran P3ATs in our study, one can conclude that the alkyl nanodomains in melt quenched samples with $6 \leq C \leq 10$ and high molecular weight are basically amorphous. There are no significant melting peaks in DSC scans at low temperatures and the polyethylene-like glass transitions α_{PE} for rreg and rran P3ATs with identical side-chain length have comparable intensity and shape. Small melting peaks in DSC heating scans slightly above room temperature are only seen for P3DDT samples (inset Figure 1e). However, the melting enthalpy ΔH_{CH2} is small, indicating that only a tiny fraction of the methylene units is crystalline. These results correspond to the findings for other nanophase-separated side-chain polymers where crystallization of alkyl groups starts to appear at comparable length.

Amorphicity of the alkyl nanodomains in rreg and rran P3ATs with $6 \leq C \leq 10$ can be explained by the fact that the alkyl groups in both series are frustrated by immobile thiophene rings in their environment and unable to pack on their native crystal lattice. At the crystallization temperature of the alkyl nanodomains, the thiophene backbones are highly immobile in all investigated P3ATs which causes serious constraints. Thiophene domains in rreg systems are crystalline while those in rran systems are in the glassy state or highly viscous since softening of the main chains occurs at T_g's between ≈ -30 °C for P3DT and 4 °C for P3HT.[18] Thus, the attachment points of the alkyl groups to the main chains do not sit on a crystalline lattice in the rran P3ATs while they are fixed to the lattice formed by the thiophene rings in rreg P3ATs. Consequently, the methylene units close to the thiophene nanodomains cannot pack easily on their own native lattice. Side-chain crystallization is usually only observed if the alkyl groups are long and flexible enough to compensate frustration effects introduced by the main

chains.[11] Crystallization of methylene sequences in the middle of the alkyl nanodomains is indicated in related systems like higher poly(*n*-alkyl methacrylates) by a nearly linear increase of crystallinity with side-chain length above a certain minimum number of CH_2 units.[49] Similar behavior seems to appear for rran and rreg P3ATs starting for $C = 12$ alkyl carbons per side chain. Crystallization of methylene sequences close to the backbone driven by that of the thiophene rings is unlikely from that perspective. Moreover, the intensities of the α_{PE} processes in rran and rreg P3ATs are quite comparable, showing that main-chain-induced crystallization is not appearing. Thiophene and alkyl nanocrystals in higher rreg P3ATs (e.g., P3DDT) are obviously decoupled by a short amorphous methylene spacer required to compensate their lattice mismatch. A similar spacer should exist between alkyl crystals and glassy main-chain domains in higher rran P3ATs like in many other semicrystalline side-chain polymers. Considering the overall situation, the crystallization tendencies of thiophene rings and alkyl side chains should compete in rreg P3ATs. This leads to nonequilibrium effects which are a driving force for long-term equilibration processes near room temperature.[38]

The four cases shown in Figure 1a can be understood as a classification scheme rationalizing the situation in nanophase-separated side-chain polymers with crystallizable main- or side-chain parts. Depending on the microstructure of the individual polymer, there can be systems where (i) side chains as well as main chains are amorphous **(mAsA)** as in melt-quenched rran P3ATs with short alkyl groups ($6 \leq C \leq 10$), (ii) the side chains are partly crystalline but the main chains are amorphous **(mAsC)** like in rran P3DDT ($C = 12$), (iii) crystalline main chains are combined with amorphous side chains **(mCsA)** as present in lower rreg P3ATs with $6 \leq C \leq 10$, or (iv) crystalline main chains combined with partly crystalline side chains **(mCsC)** as observed for rreg P3DDT ($C = 12$). Expectedly, the long-range order of the superstructure on the mesoscale is pronounced in case **mCsC** and suppressed in case **mAsA**. Interestingly, long-range order is also found for the cases **mCsA** and **mAsC**, where only one of the two subunits is (partly) crystalline. The occurrence of an ideal crystal, where both subunits are packed on one and the same lattice, seems to be unlikely for nanophase-separated polymers with comblike architecture since this requires an optimal microstructure without lattice mismatch of the subunits or a full compensation of the lattice mismatch. Whether or not this case of fully crystalline main and side chains really exists seems to be open. Such an ideal crystal would avoid the competition of two crystallization tendencies being a main reason for pronounced long-term effects[38] which seems to be characteristic for **mCsC** systems.

The most interesting finding of this work is that the dynamics in alkyl nanodomains seen as α_{PE} process is quite similar for rran and rreg P3ATs with $6 \leq C \leq 12$ alkyl carbons per side chain. This shows that the methylene units in melt-quenched samples of both series are basically amorphous and that it is seemingly unimportant for the dynamics of the CH_2 units whether the thiophene rings in their environment are amorphous or crystalline. In this sense, the α_{PE} dynamics within the alkyl nanodomains is main-chain independent. However, this does not mean that there is no interrelation between main and side chains. The side-chain length obviously affects the dynamics of the thiophene rings as confirmed by a systematic shift of the conventional α relaxation process with *C*. Recently, it was reported by Yazawa et al.[27] that the mobile alkyl groups in rreg P3HT can trigger twistlike motions of the thiophene rings being in a plastic crystalline state, i.e., sitting on a lattice but are still able to perform motions around their lattice position. In this way, the side chains can weaken the $\pi-\pi$ interaction. Whether this type of interrelation between main and side chains is a general phenomenon and of central importance for the conductivity of rreg P3ATs cannot be decided based on our results. However, it is surely an interesting topic for further investigations requiring serious information about the side-chain dynamics.

The shift of the α_{PE} process to lower relaxation temperatures $T_{\alpha_{PE},10rad/s}$ combined with a decrease of $m_{\alpha_{PE}}$ with decreasing alkyl nanodomain size has been explained previously[10] in the framework of the hindered glass transition picture.[50] Considering the α_{PE} process as dynamic glass transition in polyethylene-like matter, the observed changes are understandable as confinement effects. Changes in the cooperative dynamics are expected if the confinement size becomes comparable to the size of cooperatively rearranging regions (CRRs)[51,52] ξ_α which is characteristic length scale for the cooperative dynamics in a corresponding bulk system. According to this picture, the cooperative α_{PE} dynamics of methylene units in alkyl nanodomains should deviate from that in amorphous bulk polyethylene since the CRRs cannot reach the same size due to geometrical confinement. Deviations from the bulk dynamics should start earlier (at higher temperatures) for small domain sizes since the CRR size increases with decreasing temperature[51,53] (Figure 2f). Note that the confined α_{PE} dynamics is always faster than that in the bulk since CRR size and number of cooperatively rearranging CH_2 units are smaller. Accordingly, the steepness index $m_{\alpha_{PE}}$ indicates a transition from a cooperative α_{PE} process with non-Arrhenius-like temperature dependence for larger alkyl nanodomains to a more local β_{PE}-like process with an Arrhenius-like temperature dependence for alkyl nanodomain sizes ≤ 10 Å. Similar behavior has been reported for other series of side-chain polymers[10,44] as well as glass-forming liquids confined in nanoporous host systems with pore diameters <100 Å.[54] A remaining concern is, however, whether or not changes in the domain size are accompanied by changes in average density of the confined material.[55] Normally, it is hard to obtain detailed information about the average density of nanoconfined liquids. Thus, V_{CH2} values estimated for nanophase-separated rreg P3ATs containing amorphous alkyl nanodomains surrounded by crystalline thiophene domains are interesting. The observation is that the volume per methylene unit V_{CH2} is basically independent of side-chain length *C* and larger than the V_{CH2} volumina for crystalline lipids and polyethylene (Figure 2d). This supports the interpretation that geometrical confinement effects in domains with typical dimensions in the range 10−20 Å are the reason for the systematic shift of $T_{\alpha_{PE}}$ and a transition from Arrhenius-like to non-Arrhenius-like dynamics.

The discussion above seems to be important for an understanding of the dynamics of complex polymeric systems and can contribute to the ongoing discussion about the nature of the glass transition phenomenon.[53,56−58] Our results strongly indicate that dynamic heterogeneities connected with cooperatively rearranging regions exist and that they have typical dimensions of 10−30 Å at T_g. Much larger CRR sizes seem to be unlikely considering the results of this study and known facts about the softening behavior of nanostructured and nanoheterogeneous polymeric bulk systems in general. We think that detailed knowledge about the CRRs size is important to predict the softening behavior of multicomponent systems containing different comonomers. One single, conventional glass transition appears only if concentration profiles are averaged out within the CRR volume $V_\alpha = \xi_\alpha^3$ as commonly observed for systems which are homogeneous on the nanoscale like random copoly-

mers. Broad smeared out glass transitions appear for nanoheterogenous systems where broad interfacial regions exist causing concentration gradients on scales significantly larger than ξ_α. Consequences are CRRs having different chemical compositions resulting in multiple T_g's and a smeared out softening process as observed for gradient copolymers.[59] Two distinguishable bulk-like glass transitions will appear in nanostructured systems with domain sizes much larger than ξ_α and narrow interfaces like in microphase-separated diblock copolymers. Following this concept, one has to think about the uniformity of the chemical composition of volumes of a few cubic nanometers in order to understand peculiarities in the softening behavior of complex polymeric materials like miscible polymer blends showing two separated glass transitions[60] or proteins with a broad smeared out glass transition.[61]

Conclusions

Summarizing the results of our comparative study on P3ATs with different regularity and side-chain length, one can conclude that nanophase separation of main- and side-chain parts is a general phenomenon in such systems. Occurrence of thiophene and alkyl nanodomains with typical dimensions in the range 10−20 Å in rran as well as rreg P3ATs is indicated by (i) similarities in their side-chain crystallization behavior and (ii) a comparable α_{PE} dynamics in the alkyl nanodomains for both series independent from the packing state of the thiophene rings in their direct environment. The latter finding indicates clearly that thiophene rings and alkyl groups are demixed in rran P3ATs, despite the fact that long-range order occurs only if one type of subunits is crystalline. Accordingly, nanophase-separated side-chain polymers can be classified regarding the crystallinity of main chain and side-chain subunits. The competition of the crystallization tendencies of both phases leading to nonequilibrium situations may be the key to understand changes in macroscopic properties on long but application-relevant time scales near ambient temperature. A major finding of this work is that the α_{PE} dynamics within amorphous alkyl nanodomains changes systematically with their size, although the volume per methylene unit V_{CH2} is basically constant for rreg P3ATs with different side-chain length. This allows to separate changes in the dynamics due to geometrical confinement from effects due to packing density. The results confirm the interpretation that the commonly observed increase in α_{PE} relaxation temperature $T_{\alpha_{PE}}$ and steepness index $m_{\alpha_{PE}}$ with side-chain length are mainly due to the finite size of the alkyl nanodomains. Our observations support the existence of cooperatively rearranging regions in glass-forming polymers having typical dimensions in the range 10−30 Å at T_g. This finding is in qualitative agreement with values for the CRR size obtained from studies on small molecule liquids in nanoporous host systems as well as compatible with the softening behavior of many complex polymeric systems where an interference of structural and dynamic nanoheterogeneities should be relevant.

Acknowledgment. The authors thank Ch. Eisenschmidt for assistance with the wide-angle X-ray diffraction measurements and Th. Thurn-Albrecht and his group for stimulating discussions. Financial support by the German Science Foundation and the state Sachsen-Anhalt is gratefully acknowledged.

References and Notes

(1) Muthukumar, M.; Ober, C. K.; Thomas, E. L. *Science* **1997**, *277*, 1225–1232.
(2) Ikkala, O.; ten Brinke, G. *Science* **2002**, *295*, 2407–2409.
(3) Plate, N.; Shibaev, V. *J. Polym. Sci.: Macromol. Rev.* **1974**, *8*, 117–253.
(4) Cowie, J. M. G.; Haq, Z.; McEwen, I. J.; Velickovic, J. *Polymer* **1981**, *22*, 327–332.
(5) Ringsdorf, H.; Tschirner, P.; Hermann-Schnherr, O.; Wendorff, J. *Makromol. Chem.* **1987**, *188*, 1431–1445.
(6) Clauss, J.; Schmidt-Rohr, K.; Adam, A.; Boeffel, C.; Spiess, H. *Macromolecules* **1992**, *25*, 5208–5214.
(7) Chen, W.; Wunderlich, B. *Macromol. Chem. Phys.* **1999**, *200*, 283–311.
(8) Beiner, M.; Schröter, K.; Hempel, E.; Reissig, S.; Donth, E. *Macromolecules* **1999**, *32*, 6278–6282.
(9) Arrighi, V.; Triolo, A.; McEwen, I.; Holmes, P.; Triolo, R.; Amenitsch, H. *Macromolecules* **2000**, *33*, 4989–4991.
(10) Beiner, M.; Huth, H. *Nat. Mater.* **2003**, *2*, 595–599.
(11) Hempel, E.; Budde, H.; Höring, S.; Beiner, M. *Lecture Notes Phys.* **2007**, *714*, 201–228.
(12) Heeger, A. J. *J. Phys. Chem. B* **2001**, *105*, 8475–8491.
(13) Winokur, M. Structural studies of conducting polymers. In *Handbook of Conducting Polymers*; Skotheim, T., Elsenbaumer, R., Reynolds, J., Eds.; Marcel Dekker: New York, 1998; Vol. 2, pp 707−726.
(14) Yamamoto, T.; Komarudin, D.; Arai, M.; Lee, B.; Suganuma, H.; Asakawa, N.; Inoue, Y.; Kubota, K.; Sasaki, S.; Fukuda, T.; Matsuda, H. *J. Am. Chem. Soc.* **1998**, *120*, 2047–2058.
(15) Schopf, G.; Kossmehl, G. *Adv. Polym. Sci.* **1997**, *129*, 3–145.
(16) Arbe, A.; Genix, A.-C.; Arrese-Igor, S.; Colmenero, J.; Richter, D. *Macromolecules* **2010**, *43*, 3107–3119.
(17) Floudas, G.; Placke, P.; Stepanek, P.; Brown, W.; Fytas, G.; Ngai, K. *Macromolecules* **1995**, *28*, 6799–6807.
(18) Pankaj, S.; Hempel, E.; Beiner, M. *Macromolecules* **2009**, *42*, 716–724.
(19) Sirota, E.; Herhold, A. *Science* **1999**, *283*, 529–532.
(20) Rastogi, S.; Hikosaka, M.; Kawabata, H.; Keller, A. *Macromolecules* **1991**, *24*, 6384–6391.
(21) McCullough, R. *Adv. Mater.* **1998**, *10*, 93–116.
(22) Bao, Z.; Dodabalapur, A.; Lovinger, A. *Appl. Phys. Lett.* **1996**, *69*, 4108–4110.
(23) Sirringhaus, H.; Brown, P.; Friend, R.; Nielsen, M.; Bechgaard, K.; Langeveld-Voss, B.; Spiering, A.; Janssen, R.; Meijer, E.; Herwig, P.; de Leeuw, D. *Nature* **1999**, *401*, 685–688.
(24) Prosa, T. J.; Moulton, J.; Heeger, A. J.; Winokur, M. J. *Macromolecules* **1999**, *32*, 4000–4009.
(25) Prosa, T. J.; Winokur, M. J.; McCullough, R. D. *Macromolecules* **1996**, *29*, 3654–3656.
(26) Kline, R. J.; DeLongchamp, D. M.; Fischer, D. A.; Lin, E. K.; Richter, L. J.; Chabinyc, M. L.; Toney, M. F.; Heeney, M.; McCulloch, I. *Macromolecules* **2007**, *40*, 7960–7965.
(27) Yazawa, K.; Inoue, Y.; Shimizu, T.; Tansho, M.; Asakawa, N. *J. Phys. Chem. B* **2010**, *114*, 1241–1248.
(28) Wu, Z.; Petzold, A.; Henze, T.; Thurn-Albrecht, T.; Lohwasser, R. H.; Sommer, M.; Thelakkat, M. *Macromolecules* **2010**, *43*, 4646–4653.
(29) Chen, T.; Wu, X.; Rieke, R. *J. Am. Chem. Soc.* **1995**, *117*, 233–244.
(30) Liu, J. S.; Loewe, R. S.; McCullough, R. D. *Macromolecules* **1999**, *32*, 5777–5785.
(31) According to Scherrer, the correlation length can be estimated using $d_c = K\lambda/(w \cos \theta_{max})$ with $\lambda = 1.54$ Å being the wave length of Cu Kα radiation, K the Scherrer constant of about 1 and w the full width at half-maximum height of a reflection observed at scattering angle $2\theta_{max}$.
(32) Kawai, T.; Nakazono, M.; Sugimoto, R.; Yoshino, K. *J. Phys. Soc. Jpn.* **1992**, *61*, 3400–3406.
(33) Tashiro, K.; Ono, K.; Minagawa, Y.; Kobayashi, M.; Kawai, T.; Yoshino, K. *J. Polym. Sci., Part B: Polym. Phys.* **1991**, *29*, 1223–1233.
(34) The thickness of the thiophene layers (6 Å) is estimated based on a linear extrapolation of $d_{100}(C)$ to $C = 0$ and also independently calculated from the dimensions of thiophene rings. Both estimates are in good agreement with eachother.
(35) Small, D. M. *J. Lipid Res.* **1984**, *25*, 1490–1500.
(36) Strobl, G. *The Physics of Polymers*; Springer: Berlin, 1997.
(37) Note that it is not the focus of this work to answer the question whether the alkyl groups are "interdigitated" or "noninterdigitated" and tilted. From our current perspective, it is basically the volume V_{CH2} which determines the spacings d_{100} and d_{nps}.
(38) Pankaj, S.; Beiner, M. *Soft Matter* **2010**, *6*, 3506–3516.
(39) Heijboer, J. In *Physics of Non-Crystalline Solids*; Prins, J. A., Ed.; North Holland: Amsterdam, 1965; p 231.
(40) Meier, G.; Kremer, F.; Fytas, G.; Rizos, A. *J. Polym. Sci. B: Polym. Phys.* **1996**, *34*, 1391–1401.
(41) Mena-Osteritz, E.; Meyer, A.; Langeveld-Voss, B.; Janssen, R.; Meijer, E.; Bauerle, P. *Angew. Chem., Int. Ed.* **2000**, *39*, 2680–2684.
(42) Brinkmann, M.; Rannou, P. *Macromolecules* **2009**, *42*, 1125–1130.
(43) Lan, Y.-K.; Huang, C.-I. *J. Phys. Chem. B* **2009**, *113*, 14555–14564.
(44) Ngai, K.; Beiner, M. *Macromolecules* **2004**, *37*, 8123–8129.

(45) Johari, G.; Goldstein, M. *J. Chem. Phys.* **1970**, *53*, 2372–2388.
(46) Gopalakrishnan, T.; Beiner, M. *J. Phys.: Conf. Ser.* **2006**, *40*, 67–75.
(47) Curtis, M. D.; Nanos, J. I.; Moon, H.; Jahng, W. S. *J. Am. Chem. Soc.* **2007**, *129*, 15072–15084.
(48) Hsu, W.; Levon, K.; Ho, K.; Myerson, A.; Kwei, T. *Macromolecules* **1993**, *26*, 1318–1323.
(49) Hempel, E.; Budde, H.; Höring, S.; Beiner, M. *J. Non-Cryst. Solids* **2006**, *352*, 5013–5020.
(50) Donth, E. *Glasübergang*; Akademie-Verlag: Berlin, 1980.
(51) Adam, G.; Gibbs, J. H. *J. Chem. Phys.* **1965**, *43*, 139–146.
(52) Donth, E. *J. Non-Cryst. Solids* **1982**, *53*, 325–330.
(53) Huth, H.; Beiner, M.; Donth, E. *Phys. Rev. B* **2000**, *61*, 15092–15101.
(54) Arndt, M.; Stannarius, R.; Groothues, H.; Hempel, E.; Kremer, F. *Phys. Rev. Lett.* **1997**, *79*, 2077–2080.
(55) McKenna, G. *Eur. Phys. J.: Special Top.* **2007**, *141*, 291–301.
(56) Angell, C. *Science* **1995**, *267*, 1924–1935.
(57) Debenedetti, P. G.; Stillinger, F. H. *Nature* **2001**, *410*, 259–267.
(58) Berthier, L.; Biroli, G.; Bouchaud, J.; Cipelletti, L.; El Masri, D.; L'Hote, D.; Ladieu, F.; Pierno, M. *Science* **2005**, *310*, 1797–1800.
(59) Mok, M.; Pujari, S.; Burghardt, W.; Dettmer, C.; Nguyen, S.; Ellison, C.; Torkelson, J. *Macromolecules* **2008**, *41*, 5818–5829.
(60) He, Y.; Lutz, T.; Ediger, M.; Pitsikalis, M.; Hadjichristidis, N.; von Meerwall, E. *Macromolecules* **2005**, *38*, 6216–6226.
(61) Beiner, M. *Soft Matter* **2007**, *3*, 391–393.
(62) Ungar, G.; Zeng, X.; Brooke, G. M.; Mohammed, S. *Macromolecules* **1998**, *31*, 1875–1879.
(63) Gaur, U.; Wunderlich, B. *Macromolecules* **1980**, *13*, 445–446.

JP1072999